DEVELOPMENT OF A PILOT MODEL SUITABLE FOR THE SIMULATION OF LARGE AIRCRAFT

Mohammad M. Lone and Alastair K. Cooke
Cranfield University, Cranfield, Bedfordshire, MK43 0AL, United Kingdom

Keywords: *pilot modelling, large aircraft, aeroservoelasticity*

Abstract

Effects of aeroservoelasticity on the manual control of large civil aircraft are investigated through a pilot modelling approach based on the modified optimal control model. A synopsis of modelling techniques is presented, followed by the description of the adopted technique. A simulation environment suitable for investigating pilot-vehicle dynamics in the longitudinal axis has been developed. The derivation of the pilot model was based on limiting the bandwidth. This approach showed that the pilot-vehicle system satisfied the crossover law between 3rad/s to 10rad/s for normal acceleration response. It was found that the pilot model and the low frequency tailplane bending mode introduced a resonant peak in the pilot-vehicle frequency response that may be a cause for concern in high gain scenarios. Gust response simulations highlighted the contribution of fuselage bending mode on pilot perceived normal acceleration.

Nomenclature

e	=	perceived error
$\dot{e}$	=	perceived error rate
F_y	=	attention allocation vector
K_p	=	pilot model gain
N_{zp}	=	normal acceleration at pilot station
q	=	pitch rate
$\mathbf{Q}$	=	weightings on pilot observed variables
$\mathbf{R}$	=	weighting on control input
$\mathbf{S}$	=	weighting on rate of control input
u	=	pilot's control input
w	=	heave velocity
y	=	pilot's observed variables
Y_p	=	pilot describing function
Y_c	=	vehicle transfer function
θ	=	pitch attitude
ρ_y	=	observation noise-to-signal ratio
ρ_u	=	control input noise-to-signal ratio
τ	=	pilot's observation time delay
τ_L	=	pilot's lead time constant
τ_I	=	pilot's lag time constant
τ_n	=	neuromuscular time constant
ω_c	=	crossover frequency
ω_{BW}	=	pilot's phase bandwidth

1 Introduction

Understanding the effects of aeroservoelasticity on aircraft manual control becomes more important as airframes increase in size and flight control systems become highly sophisticated. The flight control system and low frequency aeroelastic modes can introduce significant lags into the aircraft dynamics that may degrade handling qualities. Aeroservoelastic effects on manual control has been observed on a wide variety of aircraft. The Boeing C-17A was found susceptible to lateral aircraft-pilot-coupling (APC) due to phase lags introduced by the flight control system and actuator rate limiting [1]. In the case of the Rutan Voyager, atmospheric disturbances excited a longitudinal low frequency mode that coupled symmetric wing bending with the phugoid mode [2]. These examples demonstrate the effects of sophisticated flight control systems and the aeroelastic characteristics of slender configu-

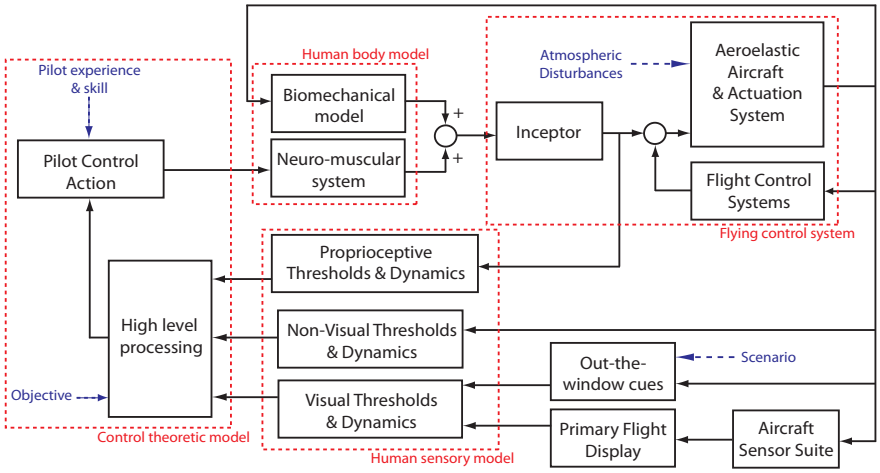

Fig. 1 Block diagram representing the pilot-vehicle-system under manual control.

rations on pilot control actions.

Supersonic transport aircraft configurations and smaller combat aircraft have attracted most of the research effort in pilot modelling and aeroservoelastics. The design process for civil aircraft relies primarily on flight simulation at later development stages. However, the need for high levels of integration between the engineering disciplines to achieve efficiency and safety goals has meant that tools for handling qualities studies that may be used at an earlier design stage are now required.

This paper presents a synopsis of pilot modelling where classical and modern approaches are compared. This is followed by the description of an optimal control based modelling technique. The development of a simulation environment where the pilot model can be coupled with an aeroelastic aircraft model for time domain simulation will be presented. The characteristics of the pilot-vehicle system in the longitudinal axis have been analysed and the results are discussed.

2 Synopsis of pilot modelling techniques

Current civil aircraft have three modes of operation. Aircraft control can be achieved through complete manual control with objectives from the pilot's mind or manual control with objectives from a flight director. The aircraft can also be controlled via the mode control panel which commands the various autopilot modes; the pilot plays a more supervisory role here. Figure 1 presents the key components involved in the manual control mode. The system is driven by an objective (derived consciously) that is subconsciously processed by higher brain functions to derive a control action; a function of pilot experience and skill. This control action is applied through the neuromuscular system that is in turn affected by the human body's response to the environment. Then it goes through the flying control system and the aircraft responds accordingly. The response is then perceived by the pilot through the various cues. Finally a control decision is made within the brain and the loop is completed.

2.1 Classical approach

One of the underlying principles in man-machine theory was proposed by McRuer during the 1960s [3]. It was called the *crossover law* and it states that the human operator adjusts his/her control action to drive the pilot-vehicle dynamics towards the following transfer function:

$$Y_p(s)Y_c(s) = \frac{\omega_c e^{-\tau s}}{s} \qquad (1)$$

where Y_p, Y_c, ω_c and τ represent the pilot transfer function, vehicle transfer function, crossover frequency and time delay respectively. Equation 1 basically states that the pilot tries to shape the

pilot-vehicle system to have an integrator like characteristic around ω_c. This has been found true for a very wide range of vehicle dynamics. ω_c is task sensitive and is also effected by the characteristics of the controlled plant. It accounts for the pilot's adaptive compensation for the vehicle dynamics. For pilots conducting compensatory attitude control tasks it has been found to lie between 1rad/s and 10rad/s [4]. The time delay is the time taken by the human body to perceive and initiate action; typically between 0.1s and 0.2s. It may be interpreted as a computational time penalty for the pilot's compensatory action.

Directly modelling human control behaviour was first attempted in 1944 by Tustin who used servomechanism theory for the analysis of manual control of anti-aircraft artillery. The following simple transfer function representation for the human operator was suggested:

$$Y_p(s) = K_p e^{-\tau s}(1+\tau_L s) \tag{2}$$

where the operator parameters K_p, τ and τ_L represent pilot introduced gain, time delay and lead respectively.

McRuer later developed the crossover model that provided a foundation for the development of various other quasi-linear models with a basic structure similar to that shown in Figure 2.

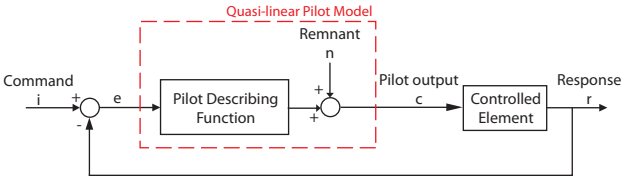

Fig. 2 Quasi-linear pilot model.

The pilot describing function is intended to represent linear behaviour whilst the remnant signal, usually a filtered Gaussian white noise, accounts for any non-linear characteristics. The key assumption is that near ω_c the pilot's linear behaviour dominates and so classical control techniques remain valid. The caveat therefore, is that the model is only accurate near ω_c.

The main appeal of such models lie in their simplicity and in the ease with which they can be analysed using classical control techniques. They have been found to be most useful for the analysis of closed loop compensatory behaviour. Equation 3 represents the quasi-linear model proposed by McRuer [5]. The pilot's gain is dependant on the task, environment and the pilot's adaptive capabilities. Pilot equalisation characteristics are represented by a lead of τ_L and a lag of τ_I. Pilot's physical reaction time and neuromuscular lag are represented by τ and τ_n respectively.

$$Y_p(s) = K_p \frac{\tau_L s+1}{\tau_I s+1}\frac{e^{-\tau s}}{\tau_n s+1} + \text{Remnant function} \tag{3}$$

The equalisation parameters are chosen such that the open loop system behaves as an integrator around ω_c; enforcing the crossover law. The gain is then tuned to fix ω_c and to make closed loop characteristics approximate those of a good feedback control system, which itself is defined by engineering judgement.

The design of the remnant function is a complicated procedure because it attempts to represent the non-linear component of pilot behaviour. It's primary source is the pilot's ability to learn and adapt which results in non-linear and non-steady behaviour. The secondary contribution comes from such things as the experimental setup and experimentally injected noise that affect pilot response to other inputs. However, careful selection of the pilot model and task can help minimise remnant effects [5].

Although the form of such models is based upon experimental results, the main disadvantage is that they are incapable of parameter variation with respect to changes in task. The model has no ability to initiate an APC event and so for their analysis sinusoidal forcing functions of varying frequencies are used to drive the system towards instability. The phase difference between the inputs and outputs is then used to predict any APC behaviour. These models also tend to be restricted to single-input-single-output analysis. Although multiple-input-multiple-output modelling can be accomplished, it is not practiced due to the increased complexity in specifying loop closures. Due to such disadvantages,

quasi-linear models, first proposed for predictive purposes, nowadays are only used for matching and validating experimental data.

2.2 Optimal control approach

The optimal control model (OCM) formulation is an algorithmic approach to pilot modelling developed by Kleinman et al in the 1970's [6]. It is based on the assumption that an experienced, well trained, highly motivated pilot will always act in an 'optimal' manner to achieve a desired goal whilst subject to inherent psycho-physical limitations. Linear optimal control theory cannot be directly applied to this problem because of the necessity to capture the effects of the time delays and remnant components inherent to the pilot. The original theoretical development showed that an estimator-predictor setup addresses this issue and yields a non-anticipative optimal control input. This setup allows the calculation of an optimal gain via the specification of a cost function, which is the sum of a fixed penalty due to the delays and the estimated states. The conceptual layout of a modified version of the OCM used in this study is presented in Figure 3.

Handling qualities analysis involving pilot models requires some form of task definition that involves a description of aircraft dynamics and usually an implicit characterisation of error in the concerned variable. For the latter, classical pilot models tend to use observable features on bode plots such as the droops and resonant peaks used in the Neal-Smith criteria. The OCM on the other hand, uses the definition of a quadratic cost function and its corresponding weighting matrices as follows:

$$J = E\left\{ \lim_{\eta\to\infty} \frac{1}{\eta} \int_0^{\eta} (\underline{y}^T \mathbf{Q} \underline{y} + \underline{u}^T \mathbf{R} \underline{u} + \dot{\underline{u}}^T \mathbf{S} \dot{\underline{u}}) dt \right\} \tag{4}$$

Here, $\underline{y}(t)$ and $\underline{u}(t)$ are vectors of pilot's observed variables and control inputs respectively. $\mathbf{Q} \geq 0$ and $\mathbf{R} \geq 0$ are the corresponding weighting matrices. The weighting matrix $\mathbf{S} \geq 0$ represents the limitations on the pilot's bandwidth due to the neuromuscular system and also a natural tendency not to perform abrupt control actions. The importance of a correct definition of this cost function cannot be understated because it lays the foundations for the derivation of pilot model transfer functions. The selection of these weightings represent the drawback of the OCM because it requires engineering judgement, experience and an iterative process. Otherwise, the algorithm certainly provides a stabilising and a robust controller representation; both qualities being characteristic of human beings in manual control.

The remaining psycho-physical limitations are modelled by the time delay, injected motor and observation noise and the Kalman estimator. The estimator attempts to capture the ability of deducing system states from perceived information. Formulation of the Kalman estimator and the calculation of the optimal gain require a model of the relevant aircraft that represents the pilot's internal model of aircraft dynamics. This should portray what the pilot expects the aircraft to behave like. Therefore, it would capture the control augmented aircraft dynamics linearised for a certain point on the flight envelope. In reality, the order of this model is a function of pilot training and experience and may include limited models of the actuation systems. The OCM approach therefore allows an explicit definition of the pilot's internal model, which may lead to a clearer understanding of pilot perceived aircraft state mismatch due to system dynamics such as aeroelasticity.

The remnant component of the quasi-linear model is represented here by observation and motor noise. These are filtered Gaussian white noise which, in the case of observation noise may be tuned to represent levels of instrument observation accuracy and the distribution of attention levels towards different instruments. It has also been shown that this approach is capable of tackling more complex systems involving visual scanning between instruments and attention-sharing by assuming that the observation noise-to-signal ratio varies directly with pilot attention towards a particular instrument [7]. The model is then completed by introducing components representing the remaining human physical limitations. These

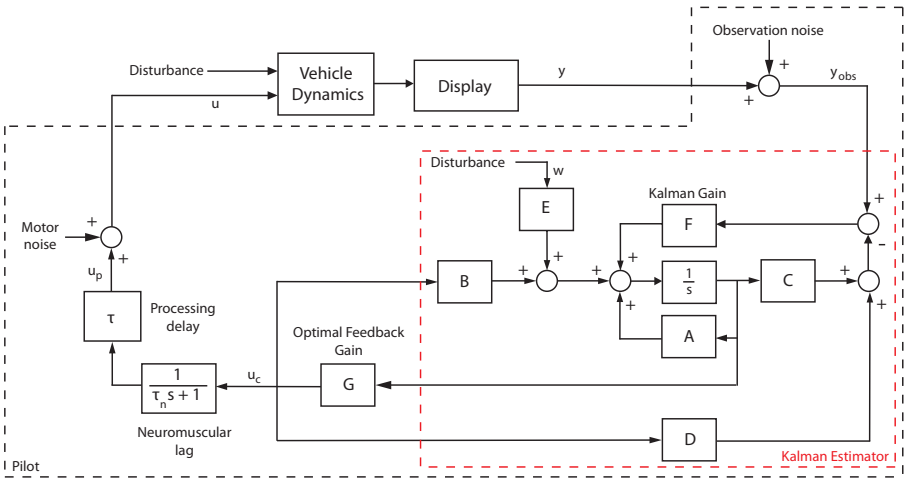

Fig. 3 Conceptual block diagram for the modified optimal control pilot model.

are the central processing time delay and neuromuscular dynamics. The latter requires explicit inclusion if the control rate component is ignored in the cost function of Equation 4.

The OCM's accuracy in matching experimental data has not been significantly superior in relation to the classical control models, indicating a degree of over-parameterisation. This has lead to a number of comparative studies with the classical models and also various attempts to simplify the OCM algorithm. The sub-optimal OCM [8] and the fixed-order OCM [9] are some results of such efforts. Both produce transfer function representations that retain the most important features for frequency domain analysis and comparison. Such studies have acted as bridges between the classical frequency domain and modern time domain approaches to the same problem. However, the complications in the simplification process far outweigh the advantages and the degree of simplification makes such models unsuitable for certain simulation purposes. Over the years, the OCM implementation has changed very little.

The OCM has mainly been applied in the analysis of time delay effects on aircraft handling qualities, such as the identification of APC prone configurations. Another area of research has been the investigation of display dynamics on the overall manual control loop and in doing so obtaining the relationship between display types and pilot ratings. The third area where the OCM has been heavily used is in the investigation of attention sharing, task interference and pilot workload. Kleinman and Baron have focused on techniques to incorporate pilot sampling behaviour based on information-theoretic ideas with the OCM [10]. This approach assumed that the pilot periodically sampled (either via his/her senses or cockpit instruments) a particular aircraft state and attempted to reconstruct it in the time domain. Another area that has received considerable focus is the attempt to relate Cooper-Harper pilot opinion rating to the OCM cost function in single and multi-axis tasks. Investigations by Hess [11] showed that the OCM cost function could be used to predict pilot opinion ratings reasonably well. The relationship was based upon the realisation that the cost function value represents the physical and mental workload of the pilot.

2.3 Modified optimal control pilot model

The MOCM is a variant of the OCM that provides a full-order pilot model, but unlike the OCM it allows for the direct calculation of the pilot model transfer functions. This modified algorithm is still capable of accounting for attention allocation and variations in neuromuscular lag. The pilot's effective time delay has been treated as a control input delay (rather than a perception delay) that allows it to be included with the vehicle dynamics for the calculation of pilot gains. This removes

$$J = E\left\{\lim_{\eta\to\infty}\frac{1}{\eta}\int_0^{\eta}\left(\begin{bmatrix} e & \dot{e}\end{bmatrix}\begin{bmatrix}1 & 0\\ 0 & 0\end{bmatrix}\begin{bmatrix} e\\ \dot{e}\end{bmatrix}+\mathbf{S}\dot{u}^2\right)dt\right\} = E\left\{\lim_{\eta\to\infty}\frac{1}{\eta}\int_0^{\eta} e^2+\mathbf{S}\dot{u}^2 dt\right\} \qquad (5)$$

the necessity to include an OCM type linear predictor. The layout of the MOCM can be seen in Figure 3. A detailed mathematical derivation of the MOCM algorithm may be found in Davidson and Schmidt [12]. A parameter variation study was conducted to observe the effects of changes in observation time delay, neuromuscular lag and attention allocation (F_y) on pilot model frequency domain characteristics. The study also provided an indirect means of verifying the in-house algorithm through comparison with what would be expected from actual pilots if these parameters were changed. A simple velocity control plant ($Y_p(s) = 1/s$) was chosen so that changes in pilot model characteristics could be observed easily. The disturbance signal was modelled as filtered Gaussian white noise with intensity 8.8. A disturbance filter of the form $1/(s+2)$ was used. Observation and control noise-to-signal ratios were set to -25dB and -20dB respectively. As pilots can perceive the rate of change alongside magnitude, the cost function includes both error (e) and error rate ($\dot{e}$). Equation 5 is the cost function used for this study.

Therefore, the following equation relates the MOCM output to the inputs:

$$\delta u(t) = \frac{\partial u(t)}{\partial e(t)}\delta e(t) + \frac{\partial u(t)}{\partial \dot{e}(t)}\delta \dot{e}(t) \qquad (6)$$

which gives the following transfer function for the pilot model:

$$\frac{u(s)}{e(s)} = \frac{u(s)}{e(s)} + s\frac{u(s)}{\dot{e}(s)} \qquad (7)$$

It is evident in Figure 4 that varying τ resulted in what would naturally be expected from a human operator. The reduction in low frequency gains with increasing τ represents prudent characteristics expected from human operators aware of their inherent time delay. Therefore, for following low frequency demands, the MOCM with a longer delay models a well motivated and well

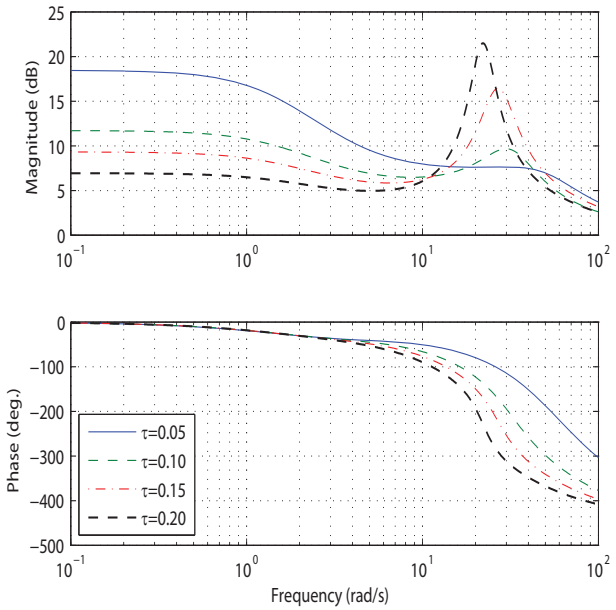

Fig. 4 Effect of varying observation time delay.

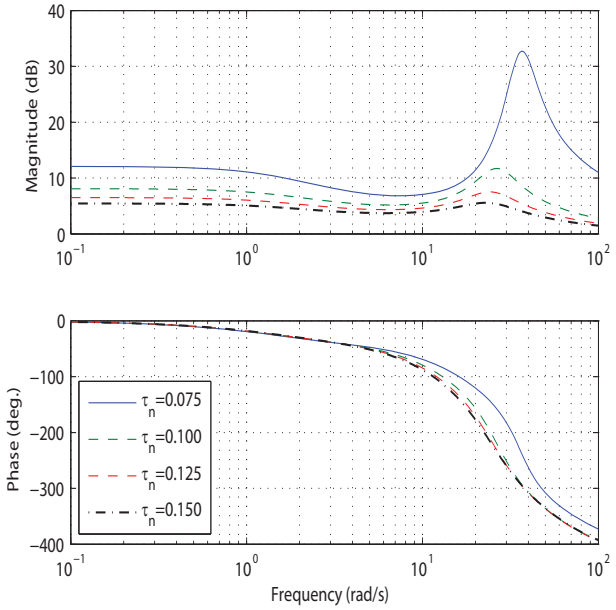

Fig. 5 Effect of varying neuromuscular lag.

trained pilot who would be cautious with control inputs. Another feature that would be expected from human pilots is that increasing τ would have a dramatic influence on the resonant peak. Here, as τ is increased the resonant peak increases in

magnitude and occurs at lower frequencies; implying long delays will lead to larger oscillations during resonance. The pilot model's phase bandwidth (ω_{BW}) can be taken as a measure of performance, i.e. how well does the model follow a demanded signal. Here, ω_{BW} has been defined as the frequency where the phase is -180°. As expected, the pilot model's ω_{BW} also decreases significantly with increases in τ, indicating that delays inhibit the pilot's high frequency performance.

The effects of varying τ_n is presented in Figure 5. Increasing τ_n has a similar effect on low frequency gains as that for τ, but not as dramatic. The opposite is found for the resonant peak where small τ_n values push the resonant peak to higher frequencies. A small τ_n also results in higher gains over the whole frequency range. Such a relation between τ_n and pilot gain implies that τ_n is inversely proportional to pilot aggressiveness. The effect on ω_{BW} is similar to that observed with variations in τ, confirming the expectation that a more aggressive pilot would have a larger bandwidth.

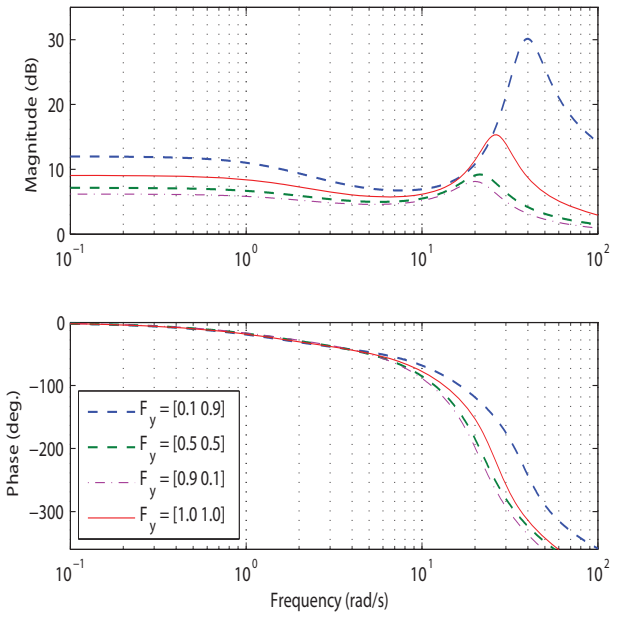

Fig. 6 Effect of varying attention allocation ($[e, \dot{e}]$).

Another parameter of interest is the attention allocation vector that models the fraction of attention allocated by the pilot to each observed variable. Figure 6 presents the changes in frequency response due to variations in this parameter. Inspecting the frequency response shows that assuming an improvement in performance (error minimisation) due to higher visibility of error is incorrect. Although the objective is to minimise error, the phase bandwidth is minimum when 90% of attention is placed on error and maximum when 90% of attention is placed on rate of change of error. This further confirms the fact that human control performance is superior when an inner error rate loop is allowed to be closed; analogous to the improvements observed when inner rate loops are implemented in flight control systems.

3 Simulation components

3.1 Aircraft model

The drive for efficiency has led to an increase in airframe size and relative reduction in airframe weight. Often as a consequence, such airframes demonstrate higher levels of structural flexibility. These structural modes may enter into the frequency range of rigid body dynamics requiring the full aeroelastic aircraft to be considered during the design of flying and handling qualities. Therefore, this study uses an aeroelastic aircraft model developed by Andrews [13] at Cranfield University. It represents a typical wide-body transport aircraft with four wing mounted engines.[1] The wing aerodynamics are captured via three dimensional vortex lattice method and ESDU data sheets were used for the fuselage aerodynamics.

For this study only twelve structural modes were included. This limited the number of system states and so improved simulation speed. Figures 7 and 8 present elevator to pitch attitude and pitch rate frequency response and also allow comparison with a reduced order rigid body model. The most prominent difference is the effect of tailplane flexibility, which is evident by the high frequency resonant peak. Consequently, a significant peak in phase is also introduced at

[1] Effects of unsteady aerodynamics have not been considered.

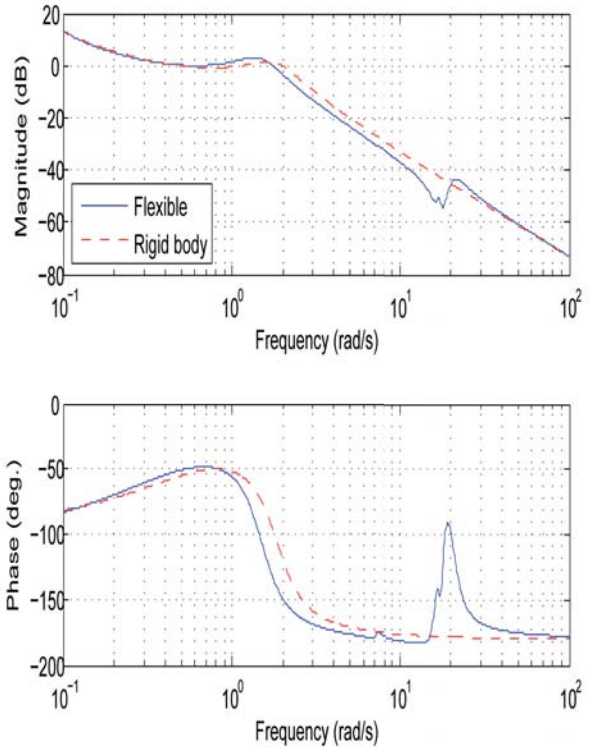

Fig. 7 Elevator to pitch attitude frequency response.

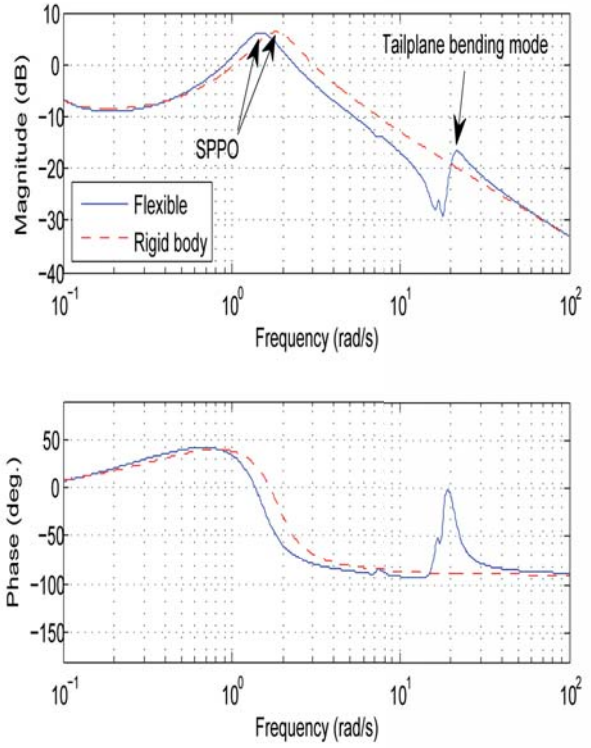

Fig. 8 Elevator to pitch rate frequency response.

Side-stick	
Spring constant, K_s	0.16°/N
Break-out force	±4N
Saturation limit	±16°
C* CSAS	
Stick command gradient, K_{sc}	0.01/degree
Pitch rate gain, K_{qc}	12.4
Command gain, K_c	0.1
Integral gain, K_i	12
Inner-loop pitch rate gain, K_q	-0.4

Table 1 Parameter values for flight control system.

that frequency. Fuselage bending modes were found to have a relatively small effect on the frequency responses. The effect on rigid body dynamics is a reduction in the aircraft's phase bandwidth and short period pitch oscillation (SPPO) mode frequency.

3.2 Flight control system

Control and stability augmentation systems (CSAS) are an essential component of modern transport aircraft. For the purposes of this study, a C* based system was implemented on the aeroelastic model along with a passive side-stick. Figure 9 presents the side-stick model and CSAS block diagram. Parameter values are shown in Table 1.

The control law defines C* as in Equation 8; a blend of normal load factor at the pilot's station (N_{zp}) and pitch rate (q).

$$\text{C*} = \frac{N_{zp}}{g} + K_{qc}q \tag{8}$$

Effectively a C* controller provides a normal load factor demand system. An inner-loop pitch rate feedback was required to improve SPPO damping.

Flight control system parameters were selected initially using frequency domain methods and then tuned through time domain simulations for the point of interest in the flight envelope. The performance of the C* CSAS can be judged via the C* criterion, which is well suited to the investigation of large aircraft handling qualities

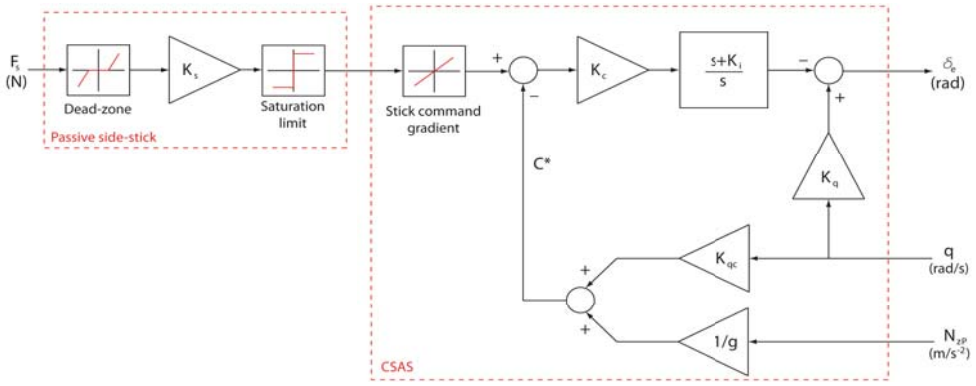

Fig. 9 Implemented inceptor model and C* control and stability augmentation system.

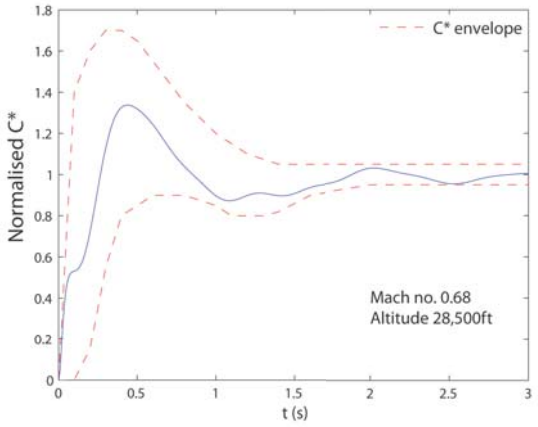

Fig. 10 Step response of C* CSAS at flight point.

because it is concerned with time domain behaviour. It requires the normalised C* step response to fit within a defined boundary. Figure 10 shows the step response for the augmented aeroelastic model. The response fits within the Level 1 handling qualities boundary.

3.3 Pilot's internal aircraft model

As mentioned earlier, the MOCM allows for an explicit definition of the pilot's internal aircraft model via the formulation of a Kalman estimator. The process of defining this model was based on the following assumptions:

- The pilot is incapable of identifying contributions of aeroelastic modes to rigid body dynamics.
- The pilot's control strategy considers the aircraft as a black box; he/she is only aware of their control input and perceived cues.

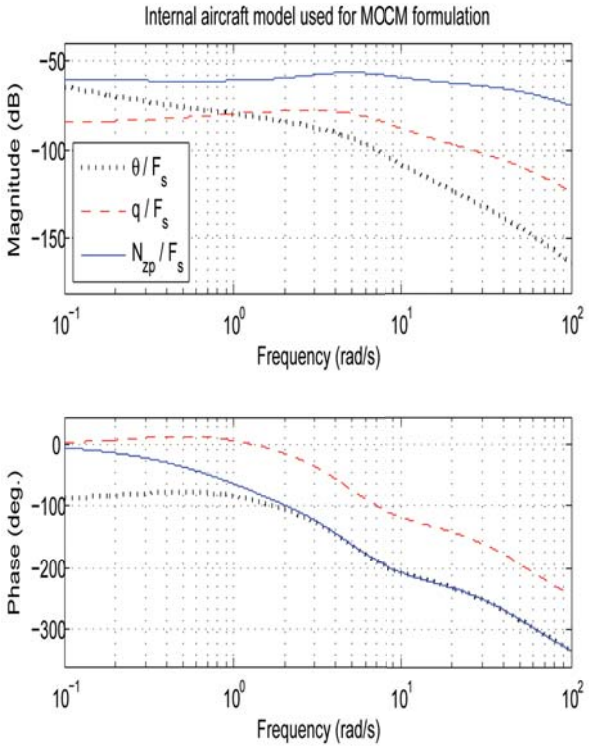

Fig. 11 Pilot's internal model frequency response characteristics.

The first step was to therefore obtain a rigid body version of the aeroelastic model. This was achieved by linearising the aeroelastic model at the point of interest in the flight envelope and then directly truncating the model from 36 to just the 12 rigid body states. The second step was to augment this model with the inceptor, CSAS

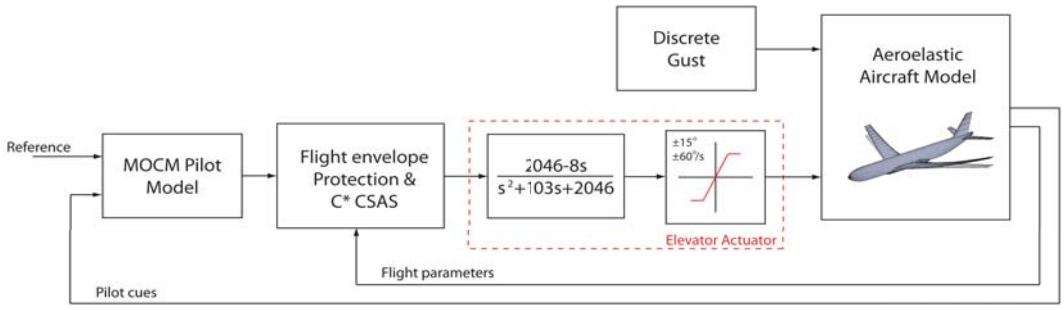

Fig. 12 Simulation environment for the pilot-vehicle system.

and actuator models. Finally, this model was linearised to yield a 21 state representation of the augmented rigid body aircraft. A balanced realisation of this model was then implemented in the MOCM algorithm. A balanced realisation is required so that well conditioned matrices are used to solve the MOCM algebraic and filter Riccati equations.

Figure 11 presents the model's stick force (F_s) to N_{zp}, q and θ frequency response.

4 Pilot-model-in-the-loop simulation

The presented components were integrated in MATLAB/Simulink for time domain simulation as shown in Figure 12. The longitudinal dynamics of the pilot-vehicle system at cruise conditions were studied (Mach 0.68 and altitude of 28,500ft).

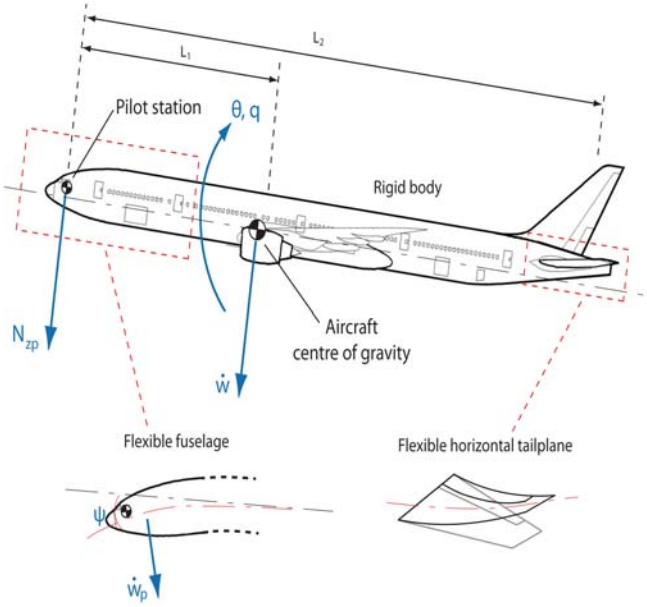

Fig. 13 Aircraft longitudinal dynamics and effects of airframe flexibility.

4.1 Selection of MOCM parameters

Although the MOCM has removed the need for careful selection of feedback signals and of pilot model gain tuning, as required for the design of quasi-linear models, it still requires careful selection of a number of parameters. Effects of varying some of these parameters were presented earlier. The task of selecting values for τ, τ_n and the noise-to-signal ratios has been made simpler by already existing empirical research in man-machine theory [6]. The values of these parameters used in this study are presented in Table 2. It was assumed that the pilot paid full attention to all three cues.

The main disadvantage in the formulation of the MOCM is the need for engineering experience and intuition for the selection of pilot perceived variables and the corresponding weightings used in the cost function. Since only longitudinal dynamics are being considered, the key variables are aircraft pitch attitude (θ), pitch rate, heave velocity (w) and cockpit normal acceleration as shown in Figure 13. Of these variables, θ, q and N_{zp} are the primary cues used by the pilot during flight [14]. N_{zp} is of particular interest here due to the large distances between the pilot's station, aircraft centre of gravity and the elevator. The effect of these parameters become clear when considering their contributions to pi-

lot perceived normal acceleration:

$$N_{zp} = (\dot{w} - L_1 \dot{q}) \cos \psi + \dot{w}_p \tag{9}$$

where $\dot{w}_p$ is acceleration due to fuselage flexibility and ψ is the fuselage pitch deflection relative to rigid body pitch attitude. L_1 is the distance between aircraft centre of gravity and the pilot's station. For large aircraft this is around 30m and so it has a significant contribution to N_{zp}. The pilot perception threshold for N_{zp} has been set to ± 0.1g [15]. No perception thresholds for θ and q have been implemented.

The weightings on θ (Q_θ), q (Q_q) and N_{zp} ($Q_{N_{zp}}$) were determined by considering their effect on the pilot model's phase bandwidth (ω_{BW}). This was found by obtaining pilot models for different combinations of weightings; all three weightings were varied logarithmically between 0.05 and 1000. It was found that ω_{BW} is primarily dependant on q feedback. On this feedback channel the weightings allocated to q and N_{zp} had the most significant effect on ω_{BW}, as shown in Figure 14. Since typically pilots can follow commands of up to 30rad/s, values of 0.1 and 3 were selected for Q_q and $Q_{N_{zp}}$ respectively. The feedback of θ and N_{zp} alongside variations in Q_θ and $Q_{N_{zp}}$ were found to have a negligible effect on ω_{BW}.

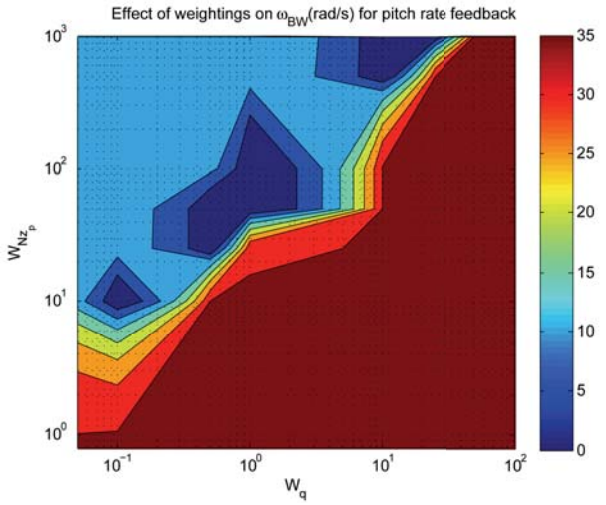

Fig. 14 Effect of W_q and $W_{N_{zp}}$ on pilot model phase bandwidth.

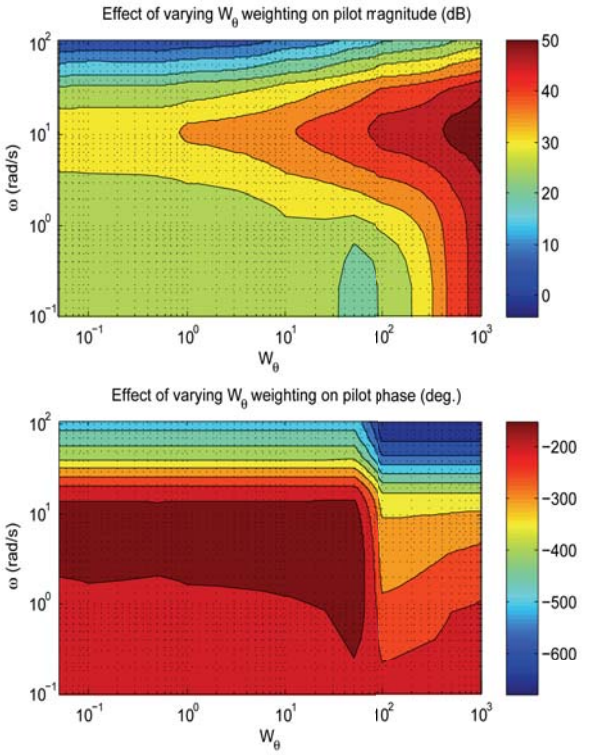

Fig. 15 Pilot model frequency response with varying W_θ for θ feedback.

After the selection of Q_q and $Q_{N_{zp}}$, effect of varying Q_θ on ω_{BW} for the three pilot cues was investigated. The only significant effect was found for θ feedback as shown in Figure 15. Therefore, a value of 60 was selected for Q_θ such that the pilot's response to changes in θ is limited to a bandwidth of around 30rad/s. Therefore, in this case the pilot's objective may be defined by the following equation:

$$J = E\left\{ \lim_{\eta \to \infty} \frac{1}{\eta} \int_0^\eta \left(60\theta^2 + 0.1q^2 + 3N_{zp}^2\right) dt \right\} \tag{10}$$

The resulting MOCM pilot model frequency domain characteristics are presented in Figure 16. The bandwidth of the pilot's response to q and N_{zp} is limited to around 11rad/s. Bandwidth for θ is much higher at around 30rad/s because of the higher weighting. Pilot model gains go up to 37dB due to the large stick forces required during manual control of large aircraft.[2]

[2]Note that the phase starts at $-180°$ due to the sign convention where pilot's pulling action is positive.

Observed cues	
Pitch attitude	θ (rad)
Pitch rate	q (rad/s)
Normal acceleration	N_{zp} (g)
Pilot limitations	
Observation time delay, τ	0.1s
Neuromuscular lag, τ_n	0.08s
Attention allocation, F_y	[1, 1, 1]
Noise-to-signal ratios	
Observation, ρ_y	-20dB
Control input, ρ_u	-25dB
Weightings	
Cues, $\mathbf{Q} = [Q_\theta, Q_q, Q_{N_{zp}}]$	[60, 0.1, 3]
Control input, **R**	0
Control-rate, **S**	0

Table 2 Pilot model parameters.

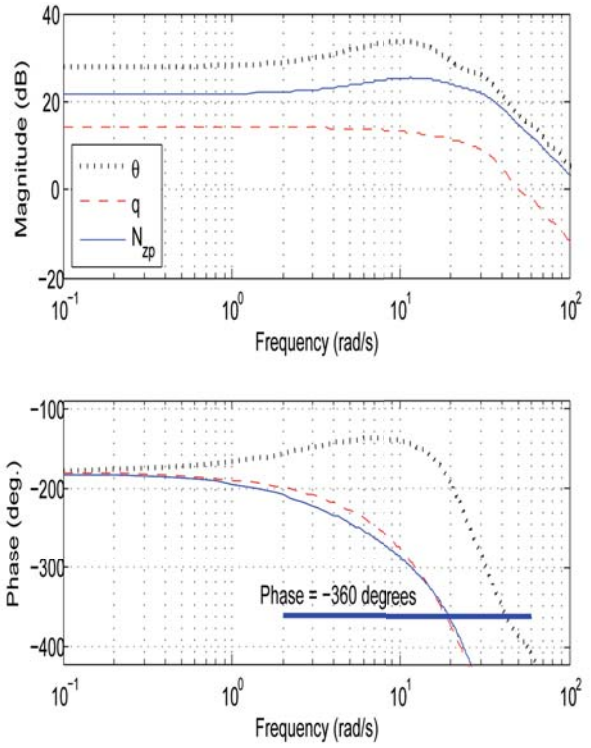

Fig. 16 MOCM pilot model frequency response.

4.2 Pilot-vehicle characteristics

Including tracking tasks with compensatory control in the MOCM formulation results in a pilot model that allows the study of the pilot-vehicle open loop dynamics.[3] Characteristics of the pilot-vehicle system to demands in pitch attitude (θ_C), pitch rate (q_C) and normal acceleration (N_{zpC}) can then be investigated. In this case the MOCM model for tracking behaviour used the same parameter values as in Table 2. Weightings on errors in θ_C, q_C and N_{zpC} were the same as Q_θ, Q_q and $Q_{N_{zp}}$.

Considering the frequency range where the pilot-vehicle system satisfies the crossover law provides an indication for the region where the pilot can easily adapt to aircraft dynamics. With regards to pitch attitude response, the crossover law is satisfied between 0.2rad/s and 1.1rad/s. Now, considering the fact that -20dB is introduced by the linear command shaping, a value of 1rad/s can be deduced for ω_c in this case. This is in agreement with the findings of Thompson and Klyde [4] and clearly points towards a system with slow dynamics in terms of attitude control (as expected from large aircraft in cruising conditions).

For N_{zp} response, the crossover law is satisfied over a larger frequency range of 3rad/s to 10rad/s. This is at higher and more desirable frequencies because the aircraft is equipped with a C* CSAS and the MOCM formulation assumes that the pilot is well trained. ω_c in this case lies at 7rad/s. Again, command shaping has meant that the magnitude response of N_zp/N_{zpC} around ω_c is near -20dB. The pilot model's attenuation of the SPPO mode is also evident as a sharp droop and slight phase lead around 1.1rad/s.

A feature evident in all three bode diagrams in Figure 17 is the high frequency resonant peak lying around the same frequency as the tailplane bending mode and the pilot model maximum gain. The assumptions when defining the pilot's internal model has meant that the pilot model provides no compensation for tailplane flexibility. This may be a cause for concern in scenarios where the pilot exhibits high gains.

[3]Tracking tasks are treated by the inclusion of error cues to the pilot model. The exclusion of tracking tasks causes the algorithm to return a pilot model in the form of a linear-quadratic regulator.

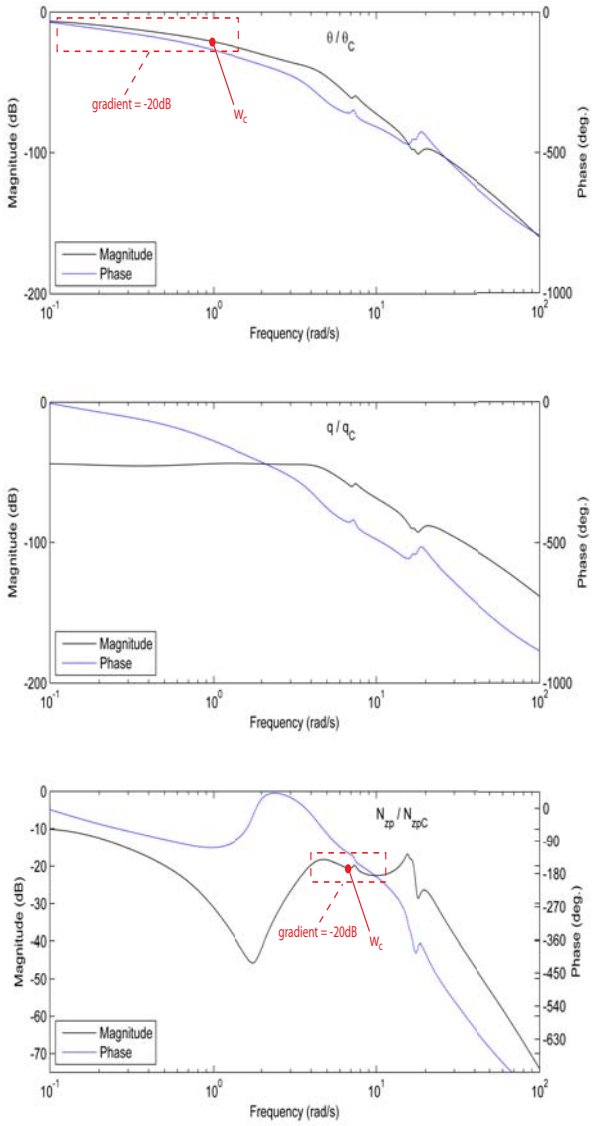

Fig. 17 Pilot-vehicle system frequency response.

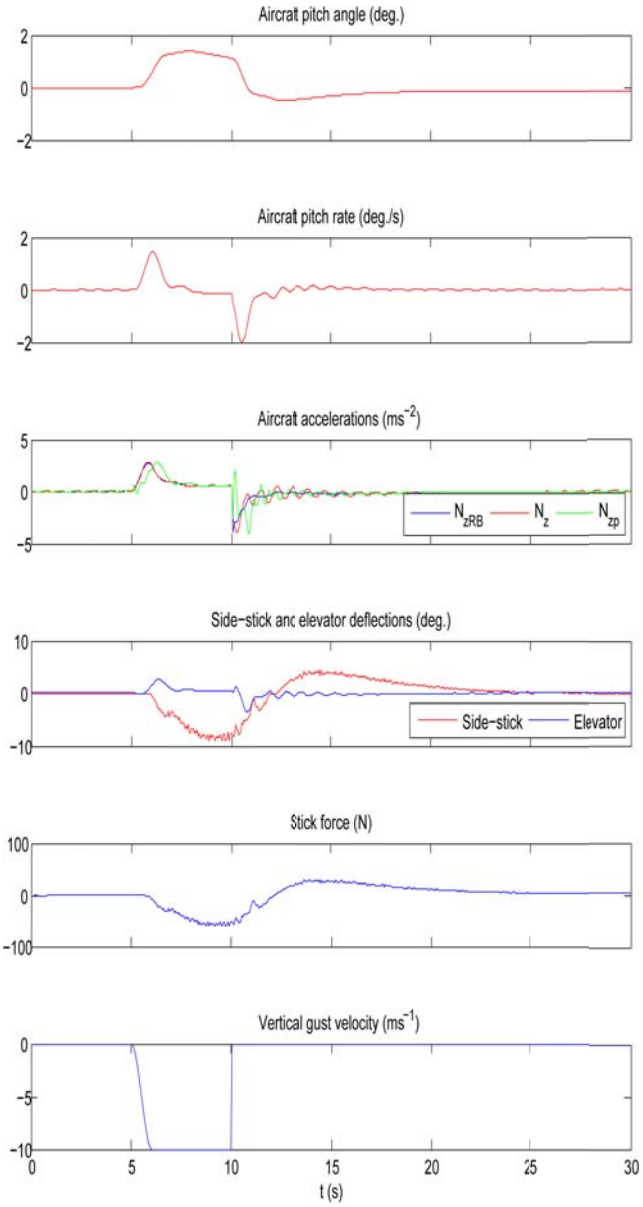

Fig. 18 Pilot-vehicle system response to a discrete gust.

4.3 Discrete gust response

Once the MOCM algorithm produces a pilot model, time domain simulations can be conducted to investigate the behaviour of the pilot-vehicle system in response to atmospheric disturbances. Here the effects of discrete gusts on aircraft dynamics during manual control are considered. The discrete gust has been modelled as velocity perturbation to aircraft centre of gravity.

Figure 18 presents the aircraft response to a discrete gust when under manual control. The gust develops over 2 seconds before sharply disappearing. The effect of the gust on aircraft pitch attitude is relatively small. On the other hand, the sharp drop in gust velocity causes a change in N_{zp} of approximately 0.7g, which consists mostly of contributions from fuselage deformation. However, the high frequency nature of this excitation has caused relatively small change in pilot input.

Although the modelling approach presented here may not provide a precise match with flight test data, it does provide a tool that can point towards possible scenarios where pilot and aircraft

dynamics may lead to undesirable outcomes.

5 Conclusions and future work

The need for high levels of design integration to achieve efficiency and safety goals has meant that tools for handling qualities studies that may be used at the early design stage are now required. This paper investigates the effects of aeroservoelasticity on the manual control of large civil aircraft.

A synopsis of pilot modelling techniques has been presented where classical and modern approaches have been compared. This is followed by the description of a pilot modelling technique based on the MOCM and the development of a simulation environment suitable for investigating pilot-vehicle dynamics in the time domain. The MOCM approach was used due to its ability to handle multiple cues and its explicit incorporation of a pilot's internal aircraft model. Effects of a discrete gust on the longitudinal dynamics have been presented to demonstrate the time domain simulation capability.

The derivation of the model was based on limiting the bandwidth of the pilot response to the percieved cues. This approach showed that the pilot-vehicle system satisfied the crossover law between 3rad/s and 10rad/s for normal acceleration response. It was found that the pilot model and the low frequency tailplane bending mode introduced a resonant peak in the frequency response that may be a cause for concern in high gain scenarios. Gust response simulation highlighted the contribution of fuselage bending mode on normal acceleration perceived by the pilot.

Although most results are as expected, the crucial future task is the validation of frequency response characteristics and time domain simulations. This will require data from either test flights or full motion simulators. Possible effects of non-linear command gradients, including the triggering of APC events are to be studied. At present, work on perception modelling, decision making and biomechanical modelling are ongoing.

5.1 Copyright Statement

References

[1] G. Weltz and K. Shweyk. Application of new and standard pilot-induced oscillation (PIO) analysis methods to flight test data of the C-17 transport aircraft. In *AIAA Atmospheric Flight Mechanics Conference and Exhibit, Hilton Head, South Carolina, Aug. 20-23, 2007*, number AIAA-2007-6387, 2007.

[2] W.J. Norton. Aeroelastic pilot-in-the-loop oscillations. In *Active Control Technology: Applications and Lessons Learned, AGARD, Turin, Italy, May 1994*, 1994.

[3] D.T. McRuer and H.R. Jex. A review of quasi-linear pilot models. *IEEE Transactions on Human Factors in Electronics*, HFE-8(3):231–249, September 1967.

[4] Peter M. Thompson, David H.Klyde, and Martin J. Brenner. Wavelet-based time-varying human operator models. In *AIAA Atmospheric Flight Mechanics, Conference and Exhibit, 6-9 August 2001 Montreal, Canada*, number AIAA-2001-4009, 2001.

[5] D.T. McRuer and E.S. Krendel. Mathematical models of human pilot behaviour. AGARDograph AGARD-AG-188, Advisory Group for Aerospace Research & Development, January 1974.

[6] D.L. Kleinman. Optimal control of linear systems with time-delay and observation noise. *IEEE Transactions on Automatic Control*, 14:524–527, October 1969.

[7] W.H. Levison. Alternative treatments of attention-sharing within the optimal control

model. In *IEEE International Conference on Systems, Man and Cybernetics*, volume 2, pages 744 – 749, Cambridge, MA, November 1989. IEEE.

[8] D.B. Doman. *Projection Methods for Order Reduction of Optimal Human Operator Models*. PhD thesis, Virginia Polytechnic Institute and State University, 1998.

[9] M. Anderson and D. Doman. Fixed order optimal pilot models. In *AIAA Guidance, Navigation and Control Conference*, number AIAA-96-3871, July 1996.

[10] D.L. Kleinman and S. Baron. The human as an optimal controller and information processor. NASA Contractor Report CR-1151, NASA, September 1968.

[11] R.A. Hess. Prediction of pilot opinion ratings using an optimal pilot model. *Human Factors*, 19:459–475, October 1977.

[12] J.B. Davidson and D.K. Schmidt. Modified optimal control pilot model for computer-aided design and analysis. Technical Memorandum 4384, NASA, Langley Research Center, October 1992.

[13] S. Andrews and A. Cooke. An aeroelastic flexible wing model for aircraft simulation. In *48th AIAA Aerospace Sciences Meeting Including the New Horizons Forum and Aerospace Exposition, Orlando, Florida, Jan. 4-7, 2010*, 2010.

[14] P.M.T. Zaal, D.M. Pool, J. de Bruin, M. Mulder, and M.M. van Paassen. Use of pitch and heave motion cues in a pitch control task. *Journal of Guidance, Control and Dynamics*, 32:366–377, 2009.

[15] R Hosman. *Pilot's Perception & Control of Aircraft Motions*. Number 90-407-1384-7. Delft University Press, November 1996.